

9th International Conference on Applied Energy, ICAE2017, 21-24 August 2017, Cardiff, UK

Numerical Modelling of the Compressible Airflow in a Solar-Waste-Heat Chimney Power Plant

Siyang Hu^a, Dennis Y.C. Leung^{a,*}

^a*Department of Mechanical Engineering, the University of Hong Kong, Hong Kong, China*

Abstract

A Solar-Waste-Heat Chimney Power Plant (SWHCPP) is similar to a solar chimney power plant (SCPP) but uses both the solar insolation and the waste heat from industries to heat the working air. To model the variation of the air density due to the high temperature rise, a 3D numerical model, in which the air density is modelled by the ideal gas law, is established for the SWHCPP in this study. Comparing with the conventional CFD model and the experimental benchmarks, the new model can suppress the overestimation in the simulated results and generally indicates an acceptable accuracy in the performance determination of the SWHCPP. In addition, a method of directly integrating the air density profiles captures the right variation in the system performance during the numerical experiment with multiple flue gas injection flow rates and it would be more suitable to be used for the modelling research about the SWHCPP. The simulations indicated that more than 50% higher power output was achieved due to multiple-stage heating with the waste heat while the existence of the waste heat slightly influenced the absorption of solar insolation.

© 2017 The Authors. Published by Elsevier Ltd.

Peer-review under responsibility of the scientific committee of the 9th International Conference on Applied Energy.

Keywords: Solar chimney; Waste heat recovery; Compressible airflow; Ideal gas law; CFD.

1. Introduction

Solar Chimney Power Plant (SCPP) uses solar insolation to generate a buoyancy-driven updraft in a chimney driving a wind turbine for electricity generation. In recent years, this system has been developed with the idea of

* Corresponding author. Tel.: +852 3917 7911; fax: +852 2858 5415.

E-mail address: ycleung@hku.hk.

coupling with the waste heat sources from industries to increase the temperature of the working air and thus improving the power output. For instance, Al-Kayiem et al. [1,2] and Chikere et al. [3] channeled hot flue gas into some tubes in or underneath the solar collector so that the working air was simultaneously heated by the solar insolation and the flue gas. Zandian et al. [4] and Zou et al. [5] put heat exchangers containing the hot recycling water from a thermal power plant at the solar collector entrance. The working air was firstly warmed by the water and then kept increasing its temperature when passing through the collector. In the design of Ghorbani et al. [6], both recycling water and flue gas were used: heat exchangers were located at the collector entrance and flue gas was injected into the chimney and mixed with the warm air from the collector. Positive outcomes were widely achieved in the studies above: the driving potential of the system was strengthened by the solar-waste-heat hybrid mode.

The studies, so far, have mainly utilized numerical simulations to illustrate the thermal-hydraulic dynamic behaviors of the Solar-Waste-Heat Chimney Power Plant (SWHCPP) and the numerical models adopted were much similar to the SCPP because the SWHCPP shares the same fundamental mechanism with the SCPP. However, a critical issue that attention should be drawn attention to is that, the incompressible Boussinesq approximation, which is widely used in the simulation on SCPPs, has a limitation on the temperature rise (ΔT) in the system, which is $\beta \cdot \Delta T \ll 1$ [7], where β is the thermal expansion coefficient of the air. However, the temperature rise in a SWHCPP would be higher than in a SCPP, especially under the scenario of injecting the flue gas into the chimney. Hence, the conventional models with the Boussinesq approximation might increase errors in the numerical outcomes. In this paper, we are going to introduce a numerical model in which the compressible air flow is simulated by using the ideal gas law to calculate the air density instead of any approximations. So that, the robustness of the model of the SWHCPP is supposed to be enhanced for a much wider ΔT range. Moreover, the simulating performance of the new compressible-air model was compared to the incompressible Boussinesq one to discuss the importance of the compressibility of the working air. Simultaneously, a novel method of estimating the driving potential of a SWHCPP is also demonstrated and found to be more suitable for the scenario of SWHCPPs.

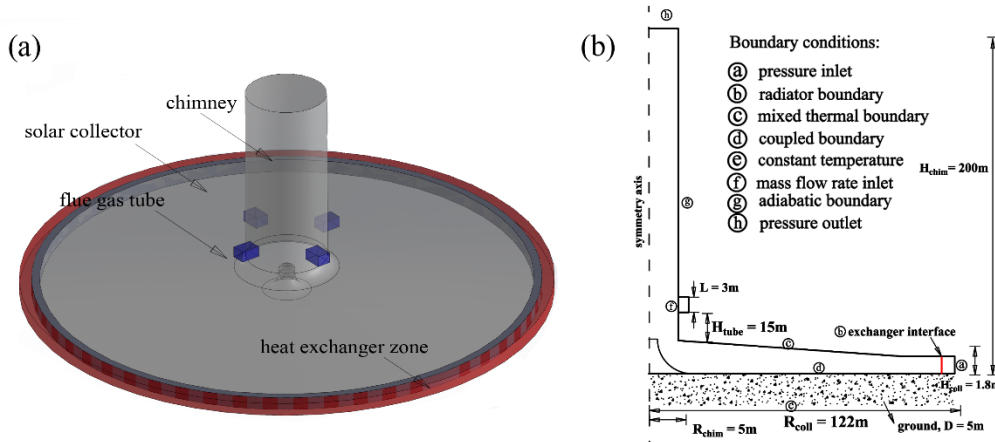


Fig. 1. The SWHCPP under simulation. (a) Schematic diagram, (b) geometry and boundary conditions in the model.

2. Methodology

2.1. The physical model of the SWHCPP

In this study, the SWHCPP used both hot recycling water and hot flue gas as the waste heat sources. Referring to the design of Ghorbani et al. [6], the heat exchangers containing the water were set in front of the solar collector but were simplified as an interface without any physical depth inside the flow domain as suggested by Zandian et al. [4], Ghorbani et al. [6] and Zou et al. [8]. The flue gas was injected directly into the chimney through four square tubes on the chimney wall. On the other hand, the solar collector and the chimney were kept consistent to the SCPP prototype

in Manzanares of Spain [9] so that we can preliminarily validate the new compressible-air model under the SCPP scenario and easily recognize the changes in the system performance when the solar-waste-heat hybrid mode is adopted. The details of the configuration are shown in Fig. 1. It should be noticed that, to save the computing resources, only one quarter of the 3D configuration was used in our simulations.

2.2. The waste heat sources

The waste heat sources used in this study were based on a practical 30MW-level waste incineration power plant in Guangdong province of China. In general, the flow rate of the recycling water from the whole plant reaches $8040 \text{ m}^3/\text{h}$ at a temperature of 43°C . As to the flue gas, the general mass flow rate is 108 kg/s and the temperature is 145°C . To compare the compressible-air model and the Boussinesq model under different ΔT conditions, the mass flow rate of the flue gas was intentionally modified to 50% (54 kg/s), 75% (81 kg/s), 150% (162 kg/s) and 200% (216 kg/s) of the general flow rate while the temperature was fixed at 145°C .

2.3. The numerical model

We used the ANSYS Fluent to simulate the 3D steady flow in the SWHCPP. The flow was generally described by the default continuity, Reynolds Averaged Naiver-Stokes (RANS) momentum, energy conservation equations in ANSYS FLUENT and the turbulence in the flow domain was modelled by the standard $k-\varepsilon$ model and the standard wall function treatment. Moreover, an additional source term, $(\rho - \rho_\infty) \cdot g$, was added in the vertical direction of the RANS equations to denote the buoyancy caused by the density difference between the working air and the ambient air. The densities in the buoyancy term and other air density in the governing equations were all modelled by the ideal gas law,

$$\rho = p/RT \quad (1)$$

For the ambient air, the pressure and temperature profiles within the chimney height were estimated by von Backstrom [10] as

$$p_\infty = p_{\infty,0} \left(1 - 0.0065H/T_{\infty,0}\right)^{5.2523} \quad (2)$$

and

$$T_\infty = T_{\infty,0} - 0.0065H \quad (3)$$

For the working air, as only the gauge pressure is computed in ANSYS FLUENT, the static pressure in Eqn. (1) was set to the sum of the gauge pressure and the ambient static pressure, p_∞ . It should be noticed that, the flue gas was treated as the air in order to avoid the additional complexity of simulating multiple species. Hence, the flue gas density also followed the ideal gas law as mentioned above. The buoyancy term and Eqns. (1) – (3) were all programmed by the User Defined Function (UDF) and compiled in ANSYS FLUENT.

For modelling the waste heat sources, 25% of the total flue gas mass flow rate was assigned to one single flue gas injection tube and the temperature was set at 145°C . As the exchangers were simplified as an interface, only the heat transferring coefficient (h in Eqn. (4)) and the pressure drop coefficient (α in Eqn. (5)) were inputted to the model and were expressed as the function of the flow velocity (v) at the exchanger interface [5,8]:

$$h = -1.3644v^4 + 24.606v^3 - 170.83v^2 + 659.19v - 6.4646 \quad (4)$$

$$\alpha = 0.0137v^4 - 0.2285v^3 + 1.417v^2 - 4.2661v - 10.328 \quad (5)$$

The other settings of the numerical model were much similar to those in our previous studies [11,12], including the boundary layer conditions (e.g. the collector roof and the solid ground), the discretization scheme and the solvers. Both the structured and unstructured grid was generated in the 3D computing domain. The grid independence test was conducted to ensure that the variation in the simulated outcomes was less than 0.1% when the number of cells changed from 1 million to 2 million.

The potential power output, P_{out} , of the simulated SWHCPP was estimated by a mathematical model [13]:

$$P_{out} = 0.5 \cdot x \cdot (1-x)^{0.5} \cdot \eta_t \cdot \Delta p \cdot V \quad (6)$$

where x denotes the pressure drop ratio at the wind turbine and the maximum power output was achieved when $x = 2/3$ [13]. V is the volume flow rate of the working air. The electricity conversion coefficient of turbine, η_t , was set to 80%. The total driving potential, Δp , was theoretically defined as

$$\Delta p = g \int_0^{H_{chim}} (\rho_\infty - \rho) dz \quad (7)$$

In the conventional incompressible Boussinesq model of SCPPs, the air density is kept constant and thus Eqn. (7) cannot be used. Instead, the gauge pressure at the chimney inlet is adopted to approximate Δp [4,6,13]. In the present model, the air density was outputted and thus we can use Eqn. (7) and integrate the air density profiles in and outside the chimney for obtaining Δp of the SWHCPP. The gauge-pressure (G.P.) method and the integration (Intg.) method were used to calculate the power output and make comparison in the following sections.

3. Validation under the scenario of the SCPP

The new compressible-air model was firstly evaluated with the experimental data of the Manzanares prototype plant since there have no experiments on the large-scale SWHCPP in literature. Three daily operating times, i.e. 8:00 am, 10:00 am and 12:00 am, were selected as the benchmarks for validating the numerical results [8,14]. Fig. 2 showed the power output deviation in the compressible-air and Boussinesq model relative to the benchmarks. Obviously, both the compressible-air and Boussinesq model overestimated the output but the new compressible model showed no more than 2 kW deviation from the experimental records. The deviation in the Boussinesq model reached 4-6 kW and over 10% higher than the experiments. Moreover, when ΔT raised from the case at 8:00 to 12:00, the difference between the compressible-air and the Boussinesq model also increased correspondingly. It implies that the Boussinesq model would induce higher overestimation in the simulated results under higher ΔT scenario. On the other hand, Fig. 2 also shows that, the power output from the integration method was very close to that of the gauge-pressure method (the difference was within 1 kW) and the benchmarks. Based on the validation above, the new compressible-air model and the integration method should be feasible for modelling the SCPP system.

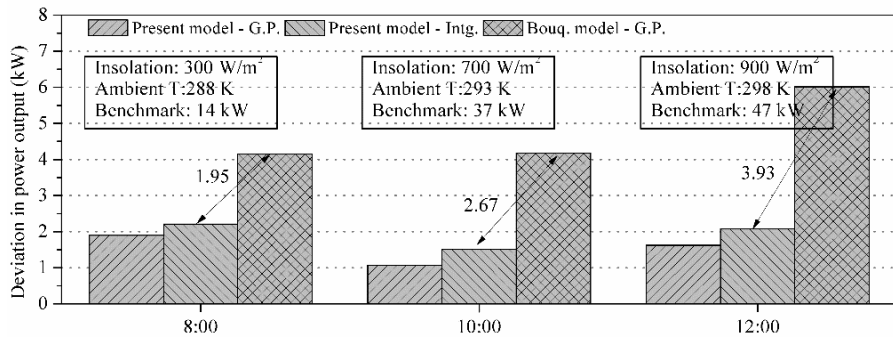


Fig. 2. Deviation in the power output between the numerical simulations and the experimental benchmarks. G.P. denotes the gauge pressure method and Intg. denotes the integration method.

4. Simulated performance of the SWHCPP

The purpose of adding waste heat is to use the waste heat to further increase ΔT inside the system and thus increase the air density difference between the ambient and the system inside, $(\rho_\infty - \rho)$. Fig. 3 illustrates the air density difference showing how this idea works on the system performance. As can be seen, both the Boussinesq and compressible-air models illustrated that, the air density difference dramatically increased in the SWHCPP cases, which should be attributed to the two-stage heating with the heat exchangers and the solar collector. In addition, the working air mixed with the hotter and lighter flue gas in the chimney and thus there was a sharp growth of the density difference nearby

the injection height of 15 m. However, the profiles from the Boussinesq model were always higher than those from the other model and indicated an unreasonable increasing trend in the profiles along the altitude, which might result in overestimation of the system performance same as the outcome in Section 3.

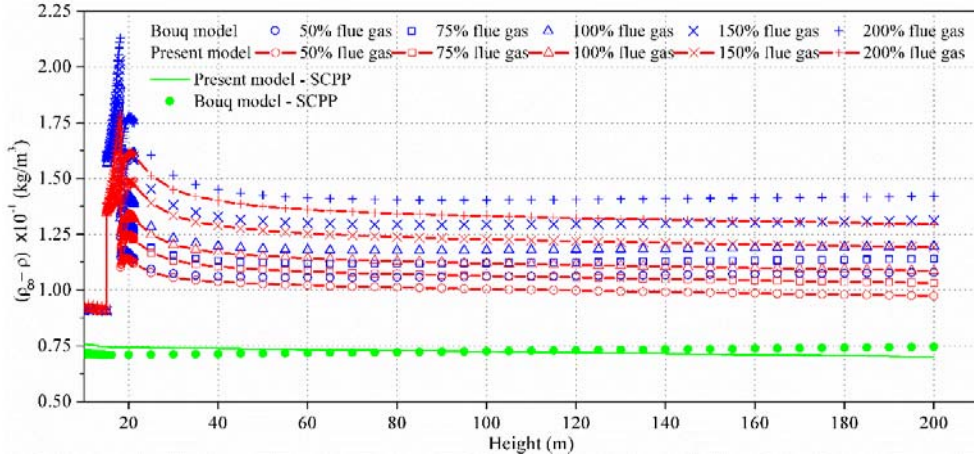


Fig. 3. Vertical profiles of the density difference between the air inside and outside the chimney.

As the density difference increased with the amount of waste heat, the power output from the SWHCPP reached more than 75 kW and was much higher than that of the SCPP (as shown in Table 1). Meanwhile, Table 1 also indicated that, the additional waste heat did not significantly affect the absorption of the solar energy while more than 50% improvement in the total ΔT was achieved. In particular, the flue gas contribution even exceeded the solar part when the flue gas flow rate was higher than 75%. It should be noticed that the recovered energy was still limited. For instance, the case of 100% flue gas flow rate obtained 1.8 MW, 7.2 MW and 9.3 MW heat from the water, solar and flue gas, respectively. The power output was only 82 kW and the efficiency was lower than 1%, which was similar to the efficiency of SCPP [8, 14]. The low-efficiency issue should be attributed to the working principle with the buoyancy [8]. Still, the SWHCPP can be a possible approach to recover the low-grade waste heat that is difficult to reuse by traditional approaches. Moreover, the efficiency could be improved with some structural innovations [11, 12] that were already evaluated in SCPPs.

Table 1. Performance of the SWHCPPs with different flue gas flow rates and the contributions of the multiple heat sources.

Flue gas flow rate	P_{out} (kW)	Total ΔT (K)	Recycling water		Solar insolation		Flue gas	
			ΔT (K)	Contribution	ΔT (K)	Contribution	ΔT (K)	Contribution
SCPP	49	21.6	--	--	21.6	100%	--	--
50%	75	50.8	5.7	11.3%	20.6	40.4%	24.5	48.3%
75%	79	53.2	5.7	10.8%	20.6	38.8%	26.8	50.4%
100%	82	55.3	5.8	10.4%	20.8	37.5%	28.8	52.1%
150%	89	59.0	5.8	9.8%	21.1	35.7%	32.2	54.6%
200%	94	62.4	5.8	9.2%	21.4	34.3%	35.2	56.4%

The power outputs in Table 1 were calculated with the integration method and the growing trend over the multiple flue gas flow rates was consistent to the results in the Fig. 3 and the changes in the total ΔT . However, the power outputs, which were based on the chimney inlet gauge pressure, indicated a decreasing tendency (not shown here). It should be recognized that, the gauge pressure at the chimney inlet is just related to the air flow from the collector while there is another branch of flow, i.e. the flue gas, in the system. Hence, the chimney-inlet gauge pressure might

only represent a part of the total driving potential in the SWHCPP. The integration method is proceeded with the whole vertical air column by following the definition of driving potential and thus should be more accurate for estimating the potential power output of the SWHCPP.

5. Conclusion

A 3D numerical model was established for simulating the compressible airflow in the SWHCPP in this study. The compressibility of the fluids inside the system was modeled by the ideal gas law that was programmed by the UDF in ANSYS FLUENT. The simulating performance of the new model was validated with the experiments and compared with the conventional Bouqssinesq model. The results indicated that the compressible-air model is feasible for modelling the buoyancy-driven flow in the SCPP as well as the SWHCPP and can suppress the overestimation in the results compared with the Bouqssinesq model.

Simultaneously, the air density profiles inside and outside the chimney were integrated directly to estimate the driving potential based on the new compressible-air model. For the SCPP, this integration method showed a comparable accuracy with the conventional method used in literature while, for the SWHCPP, this method was found to be more accurate during the numerical experiment with flue gas injection to enhance its performance.

Preliminary simulations on the SWHCPP indicated that more than 50% higher power output was achieved with the additional waste heat. Moreover, the contribution of flue gas to the total ΔT was comparable to the solar part while the existence of the waste heat influenced slightly the absorption of solar insolation.

In this study, the new simulating tools were found to be feasible for simulating the SWHCPPs with different configuration designs and conditions of waste heat sources. Subsequent research would be conducted in the future to further understand the thermal-hydraulic dynamic behavior of the SWHCPP and optimize the system for possible industrial applications.

Acknowledgements

This project is funded by the CRCG (a/c 104003483) of the University of Hong Kong.

References

- [1] Al-Kaiyem H.H., Yin K.Y., Sing C.Y. Numerical simulation of solar chimney integrated with exhaust of thermal power plant. WIT Press: United Kingdom, 2012.
- [2] Al-Kaiyem H.H., Gilani S.I. Simulation of a collector using waste heat energy in a solar chimney power plant system. WIT Transactions on Ecology and the Environment 2013;179:933-944.
- [3] Chikere A.O., Alkaiyem H.H., Karim Z.A.A. Thermal field study and analysis in hybrid solar flue gas chimney power plant. National Postgraduate Conference (NPC), IEEE 2011;p.1-6.
- [4] Zandian A., Ashjaee M. The thermal efficiency improvement of a steam Rankine cycle by innovative design of a hybrid cooling tower and a solar chimney concep. Renewable energy 2013;51:465-473.
- [5] Zou Z., He S. Modelling and characteristics analysis of hybrid cooling-tower-solar-chimney system. Energy Conversion and Management 2015;95:59-68.
- [6] Ghorbani B., Ghashami M., Ashjaee M., et al. Electricity production with low grade heat in thermal power plants by design improvement of a hybrid dry cooling tower and a solar chimney concept. Energy Conversion and Management 2015;94:1-11.
- [7] ANSYS FLUENT, Release 14.0 User's Guide, 2011, ANSYS Inc., Canonsburg, Pennsylvania.
- [8] Haaf W., Friedrich K., Mayr G., et al. Solar chimneys part I: principle and construction of the pilot plant in Manzanares. Int. J. of Solar Energy 1983;2(1):3-20.
- [9] Zou Z., Gong H. Numerical analysis of solar enhanced natural draft dry cooling tower configuration. Applied Thermal Engineering 2016;94:697-705.
- [10] von Backstrom, T.W., Gannon, A.J. Compressible flow through solar power plant chimneys. J. Solar Energy Engineering 2000;122:138–145.
- [11] Hu S.Y., Leung D.Y.C., Chen M.Z.Q., et al. Effect of guide wall on the potential of a solar chimney power plant. Renewable Energy 2016;96:209-219.
- [12] Hu S.Y., Leung D.Y.C., Chan J.C.Y. Impact of the geometry of divergent chimneys on the power output of a solar chimney power plant. Energy 2017;120:1-11.
- [13] Koonsrisuk A., Chitsomboon T. Mathematical modeling of solar chimney power plants. Energy 2013;51:314-322.
- [14] Haaf W. Solar chimneys part II: preliminary test results from the Manzanares pilot plant. Int. J. of Sustainable Energy 1984;2(2):141-161.